Communications in Physics, Vol. 28, No. 3 (2018), pp. 237-245
DOI:10.15625/0868-3166/28/3/12666

GROWTH OF SINGLE CRYSTALS OF METHYLAMMONIUM LEAD MIXEDHALIDE PEROVSKITES

THUAT NGUYEN-TRAN[a,†], NGOC MAI AN[a], THU TRANG LUONG[b], HUNG HUY NGUYEN[b] AND THANH TU TRUONG[b]

[a]*Nano and Energy Center, VNU University of Science, 334 Nguyen Trai, Thanh Xuan District, Hanoi, Vietnam*

[b]*Faculty of Chemistry, VNU University of Science, 19 Le Thanh Tong, Hoan Kiem District, Hanoi, Vietnam*

[†]*E-mail:* thuatnt@vnu.edu.vn

Received 11 June 2018
Accepted for publication 23 July 2018
Published 31 August 2018

Abstract. *We report the growth and characterization of different bulk single crystals of organo lead mixed halide perovskites $CH_3NH_3PbI_{3-x}Br_x$ by two different crystal growth approaches: (i) anti-solvent diffusion, and (ii) inverse temperature crystallization. In order to control the size and the shape of crystals, we have investigated different experimental growth parameters such as temperature and precursor concentration. The morphology of obtained crystals was observed by optical microscope, whereas their intrinsic crystalline properties were characterized by single crystal as well as powder X-ray diffraction. The results illustrated that the growth and crystalline structure of mixed halide perovskites $CH_3NH_3PbI_{3-x}Br_x$ could be easily tuned.*

Keywords: Organo lead mixed halide perovskites, single crystal, $CH_3NH_3PbI_{3-x}Br_x$.

Classification numbers: 61.05.C-; 81.05.Hd.

I. INTRODUCTION

Until now, the power conversion efficiency of hybrid organo metal halide perovskite solar cells has significantly increased up to 20.1% [1]. These up-to-the-minute new devices surpassed other third-generation solar cells to become the most promising rival to the silicon-based solar cells due to their superiorities, such as high charge carrier motilities, low temperature (below 150˚C) solution process, extreme large carrier diffusion lengths, as well as the outstanding photovoltaic efficiencies [2–4]. Since the morphology of the perovskite lm is one of the most crucial factors to aect the performance of the device, many approaches have been developed for its improvement. Well-controlled morphology of the perovskite layer is a significant element to provide the device with high efficiency and high stability. In order to improve quality of the perovskite layer, various techniques have been reported such as additives, [5,6] fast deposition-crystallization (anti-solvent dripping), [7,8] sequential deposition method [9], hot casting technique [10], nonstoichiometric perovskite precursor [11], and vapor-assisted annealing [12]. Since monocrystalline-based solar cells always possess the potential of yielding higher power conversion efficiency than multicrystalline-based ones, understanding the growth mechanism of perovskite crystallites has great benets for further improving the performance and enlightening us to exploit new technologies for large-scale and low-cost fabrication of perovskite solar cells. In this paper, we report the investigation of the growth and characterization of bulk single crystals of $CH_3NH_3PbI_{3-x}Br_x$ perovskites. The general morphology of the obtained single crystals was observed by optical microscope, whereas their crystalline structures were characterized by X-ray diffraction techniques.

II. EXPERIMENTAL PROCEDURES

II.1. Preparation of Precursors CH_3NH_3I and CH_3NH_3Br

CH_3NH_3I was synthesized by the equimolar reaction between CH_3NH_2 25 wt.% in ethanol and HI 57 wt.% in water at 0˚C in 2 h under nitrogen purge. CH_3NH_3Br was synthesized by the equimolar reaction between CH_3NH_2 25 wt.% in ethanol and HBr 40 wt.% in water at room temperature in2 h under nitrogen purge. The crystallization of CH_3NH_3I or CH_3NH_3Br was carried out by rotary evaporation of the corresponding solutions. The obtained crystals were washed in diethyl ether, and then dried in vacuum at 60˚C.

II.2. Preparation of $CH_3NH_3PbI_{3-x}Br_x$ Solutions

In order to prepare the solution of $CH_3NH_3PbI_3$ in gamma-Butyrolactone (GBL) 1M, an equimolar mixture of PbI2 (2.305g) and CH_3NH_3I (0.795g) was diluted in GBL solvent by stirring. The mixture was then kept at 60˚C for 3 h until the mixture became yellow and clear. Finally, the solution was transferred into a glass vial and kept at room temperature. The solution of $CH_3NH_3PbBr_3$in dimethylformamide (DMF) 1Mwas prepared by similar way from an equimolar mixture of 1.835g $PbBr_2$ (white powder), 0.56g CH_3NH_3Br (white crystal) and DMF solvent.

II.3. Growth of $CH_3NH_3PbI_{3-x}Br_x$ Perovskitesingle Crystals

For the growth of single crystals via the anti-solvent diffusion (ASD) method [13], 5 ml of $CH_3NH_3PbI_{3-x}Br_x$solutionwas filtered through a 0.2 μ PTFE syringe filter and placed in a small open vial and then put into a bigger and sealed container with 7 ml of dichloromethane (DCM),acting as anti-solvent. The experimental setup was kept overnight at room temperature

and under normal atmospheric pressure. DCM, which is more volatile, was naturally evaporated, and diffused from the gaseous phase into the precursor solution, leading to supersaturation, then nucleation and finally crystallization. We can regulate the diffusion speed by varying the temperature. For the inverse temperature crystallization (ITC) method [14], 3 ml of $CH_3NH_3PbI_{3-x}Br_x$solutionwas filtrated through a 0.2 μm PTFE syringe filter and placed into a sealed glass vial. The solution was then heated to 110°C in an oil bath until the first crystal appearance and kept for another 3 h. These single crystals were then taken out with a spoon and kept in DCM for protecting from moisture.

II.4. Characterization

To determine the site and position of each atom in the perovskite unit cell, we used single-crystal X-ray diffraction (SCXRD) measurement with Mo-Kα radiation ($\lambda = 0.71073$Å). In parallel, we used powder X-ray diffraction (XRD) measurement, on a Bruker D8 Advance X-ray diffractometer with Cu-Kα radiation ($\lambda = 1.5418$Å, 2θ steps $= 0.03^\circ$/step). General shapes and morphology of the obtained crystals was investigated by an optical microscope with different magnification.

III. RESULTS AND DISCUSSION

The general information of five different large bulk single crystals of $CH_3NH_3PbI_{3-x}Br_x$ ($x = 0$, 1, 2, 2.75 and 3) is shown in Table 1. The value of x, so called the preparation ratio, is calculated from the volume ratio of 1 M $CH_3NH_3PbI_3$ solution in GBL and 1 M $CH_3NH_3PbBr_3$ solution in DMF, more precisely, the preparation ratio $x = 3 \times V_{CH_33NH_3PbI_3} / (V_{CH_3NH_3PbI_3} + V_{CH_3NH_3PbBr_3})$. The color of synthesized single crystals changes from black, at $x = 0$, to blackish brown, at $x = 1$, to orange, at $x = 2$, 2.75, and 3. The morphology of these large single crystals changed from parallelogram blocks, at $x = 0$, to hexagonal one, at $x = 1$, and cubic one, at $x = 2$, 2.75, 3.

Table 1. The general information of single crystals of mixed halide perovskites.

No.	Preparation formula	Preparation ratio x	$CH_3NH_3PbI_3$/ $CH_3NH_3PbBr_3$	Color	Bulk crystal morphology	Size
1	$CH_3NH_3PbI_3$	0	3:0	black	parallelogram	0.5 mm × 1 mm
2	$CH_3NH_3PbI_2Br$	1	2:1	dark brown	hexagonal	1.5 mm × 1.5 mm
3	$CH_3NH_3PbIBr_2$	2	1:2	orange	cubic	2 mm × 2 mm
4	$CH_3NH_3PbI_{0.25}Br_{2.75}$	2.75	1:11	orange	cubic	1.5 mm × 1.5 mm
5	$CH_3NH_3PbBr_3$	3	0:3	orange	cubic	2 mm × 2 mm

Fig. 1a illustrates that the color of crystals changes from orange color (for high content of bromide) to more and more blackish brown color when the content of bromide reduces. Fig. 1b shows that large single crystals with the size of about 2 mm to 3 mm have been successfully synthesized.

Characterization using an optical microscope is a simple way to quickly observe the size, the shape, and the morphology of obtained single crystals. Fig. 2 shows the optical images of the single crystals of perovskites with preparation formulas: (a) $CH_3NH_3PbI_3$, (b) $CH_3NH_3PbI_2Br$, (c) $CH_3NH_3PbI_{0.25}Br_{2.75}$, (d) $CH_3NH_3PbIBr_2$ and (e) $CH_3NH_3PbBr_3$.

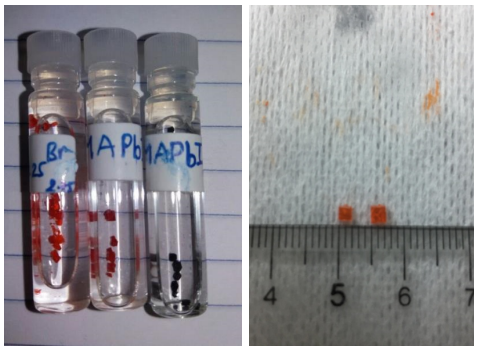

(a) (b)

Fig. 1. (a) $CH_3NH_3PbI_{3-x}Br_x$ crystals with preparation ratio $x = 2.75$, 2, to 1 (going from left to right) (b) $CH_3NH_3PbBr_x$ crystal (2 mm $\times$ 2 mm).

The sharp edges of the obtained crystal illustrate the uniform growth of those single crystals. When one iodide atom is replaced by one bromide atom in the perovskite unit cell, single crystals of $CH_3NH_3PbI_2Br$ are obtained with the dimension of 1.5 mm $\times$ 1.5 mm in hexagonal shapes. As the content of bromide increased, the shape of the obtained crystals is more and more associated with the cubic shape as illustrated in Fig. 2c for the single crystal of $CH_3NH_3PbIBr_2$ with the dimension of 2 mm $\times$ 2 mm.

Table 2. X-ray structure data collection and refinement parameter of single crystal perovskites with preparation formula $CH_3NH_3PbI_3$, $CH_3NH_3PbI_2Br$, $CH_3NH_3PbI_{0.25}Br_{2.75}$ and $CH_3NH_3PbBr_3$.

Preparation formula		$CH_3NH_3PbI_3$	$CH_3NH_3PbI_2Br$	$CH_3NH_3PbI_{0.25}Br_{2.75}$	$CH_3NH_3PbBr_3$
Refined formula		$CH_3NH_3PbI_3$	$CH_3NH_3PbI_{1.69}Br_{1.31}$	$CH_3NH_3PbI_{0.13}Br_{2.87}$	$CH_3NH_3PbBr_3$
Crystal System		tetragonal	cubic	cubic	cubic
Space group		I4/mcm	Pm-3m	Pm-3m	Pm-3m
Z		32	48	48	48
Volume (Å^3)		999.34(15)	229.73(5)	209.55(5)	208.63(6)
Lattice parameter	a (Å)	8.8850(6)	6.1245(4)	5.9397(5)	5.931(1)
	b (Å)	8.8850(6)	6.1245(4)	5.9397(5)	5.931(1)
	c (Å)	12.6590(9)	6.1245(4)	5.9397(5)	5.931(1)
	$\alpha(^\circ)$	90	90	90	90
	$\beta(^\circ)$	90	90	90	90
	$\gamma(^\circ)$	90	90	90	90

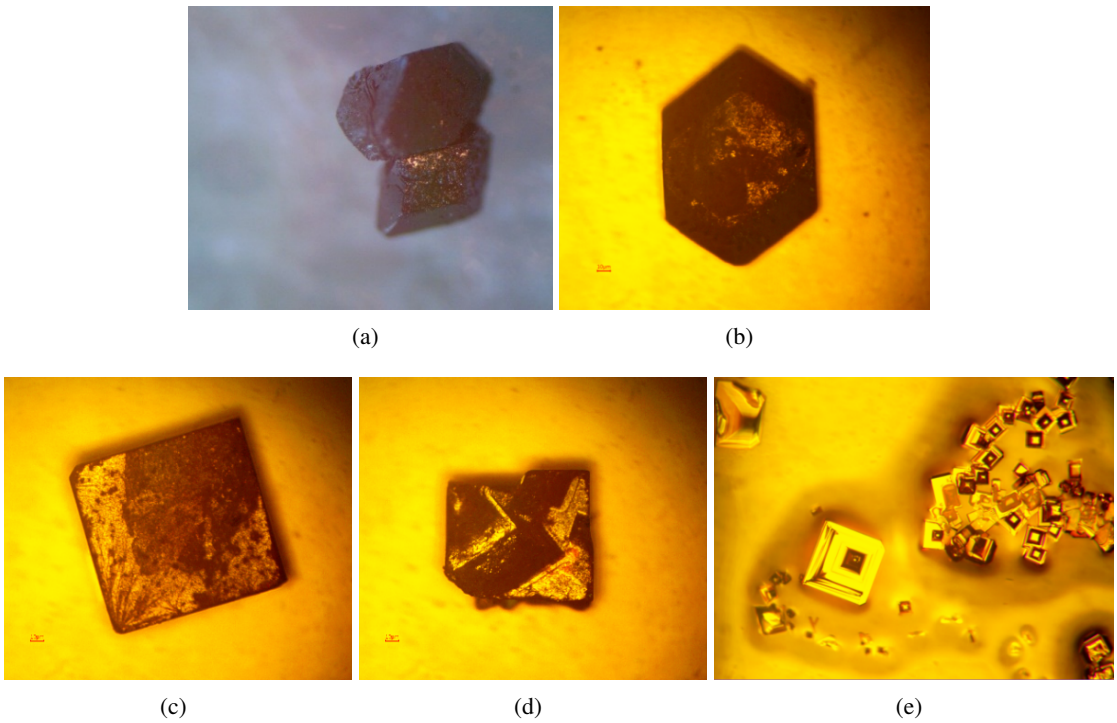

Fig. 2. The optical images of preparation formulas (a) $CH_3NH_3PbI_3$, (b) $CH_3NH_3PbI_2Br$, (c) $CH_3NH_3PbIBr_2$, (d) $CH_3NH_3PbI_{0.25}Br_{2.75}$ and (e) $CH_3NH_3PbBr_3$ crystals with a magnification of 4X.

In order to investigate the structure and the purity, the obtained material has been investigated by XRD measurements of the powder samples. SC-XRD measurements have also been carried out on well selected perovskite single crystals. Structural parameters of perovskites, deduced from the refinement of SCXRD data, are summarized in Table 2. The diffraction patterns in good agreement with simulated and literature data[15] correspond to the respective conformation of the perovskites structure: tetragonal for $CH_3NH_3PbI_3$ as showed in Fig. 3, cubic for $CH_3NH_3PbI_2Br$ (Fig. 4), $CH_3NH_3PbI_{0.25}Br_{2.75}$ (Fig. 5) and $CH_3NH_3PbBr_3$ (Fig. 6).

The difference of structures leads to the difference in the orientation of CH_3NH_3+. In the tetragonal structure of $CH_3NH_3PbI_3$, according to the refinement of SCXRD data, the nitrogen atom is at the center, and the carbon is disordered in 4 different positions around the nitrogen atom. These positions are related through symmetry operations of 2/c (parallel to b axis) and 2 (parallel to c axis). In the cubic structure of $CH_3NH_3PbBr_3$, the carbon atom and nitrogen atom are substitutionally disordered. Each atom is equally occupied 6 positions which are related through symmetry operations of 3 parallel to [1,1,1] and inversion center resulting in 6 possible orientations of CH_3NH_3+ ion. This model is refined without adding hydrogen atoms. The methylammonium lead mixed halide perovskite (the preparation formula $CH_3NH_3PbI_2Br$ with the corresponding SCXRD refined formula $CH_3NH_3PbI1.69Br1.31$, and the preparation formula $CH_3NH_3PbI_{0.25}Br_{2.75}$ with the corresponding SCXRD refined formula $CH_3NH_3PbI0.13Br2.87$),

has similar cubic structure in which halide ions are substitutionally disordered and occupied similar positions of bromide ions in $CH_3NH_3PbBr_3$. Bonding situation of CH_3NH_3+ ion in these two perovskites is similar to that described in $CH_3NH_3PbBr_3$.

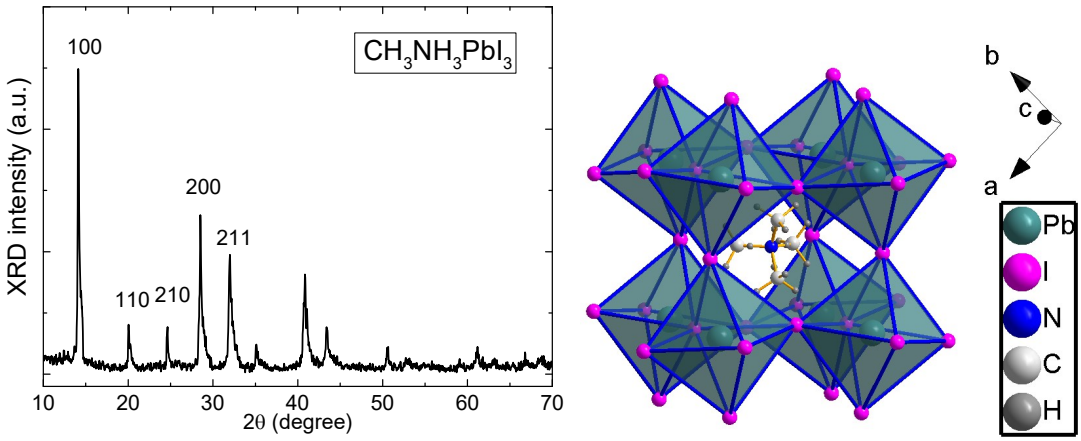

Fig. 3. (a) Experimental XRD pattern of $CH_3NH_3PbI_3$ powder, and (b) corresponding SCXRD refined structure model of $CH_3NH_3PbI_3$ single crystal with tetragonal structure. Four possible orientations of CH_3NH_3+ ion, related through different symmetry operations, are presented.

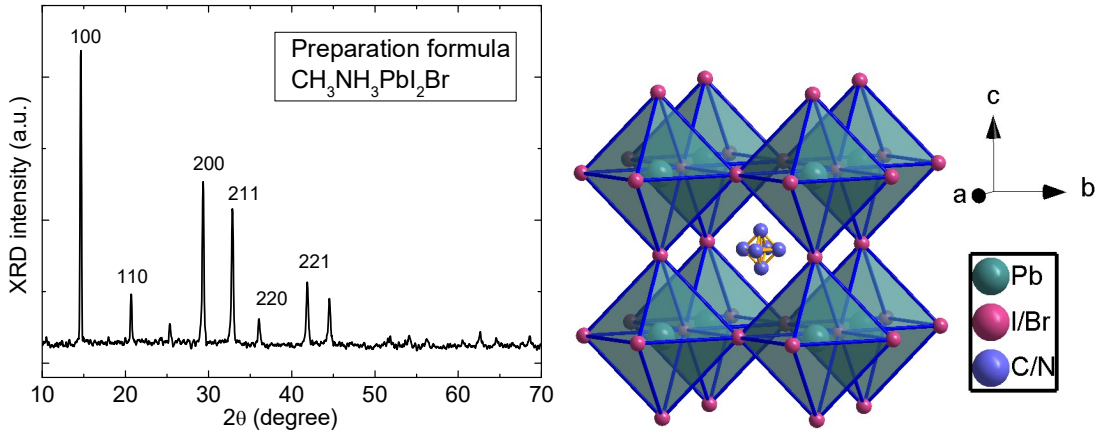

Fig. 4. Experimental XRD pattern of preparation formula $CH_3NH_3PbI0.25Br0.75$ powder, and (b) corresponding SCXRD refined structure model of $CH_3NH_3PbI1.69Br1.31$ single crystal with cubic structure. Six possible positions, equally occupied by C or N, related through different symmetry operations, are presented. Hydrogen atoms were not added for the refinement.

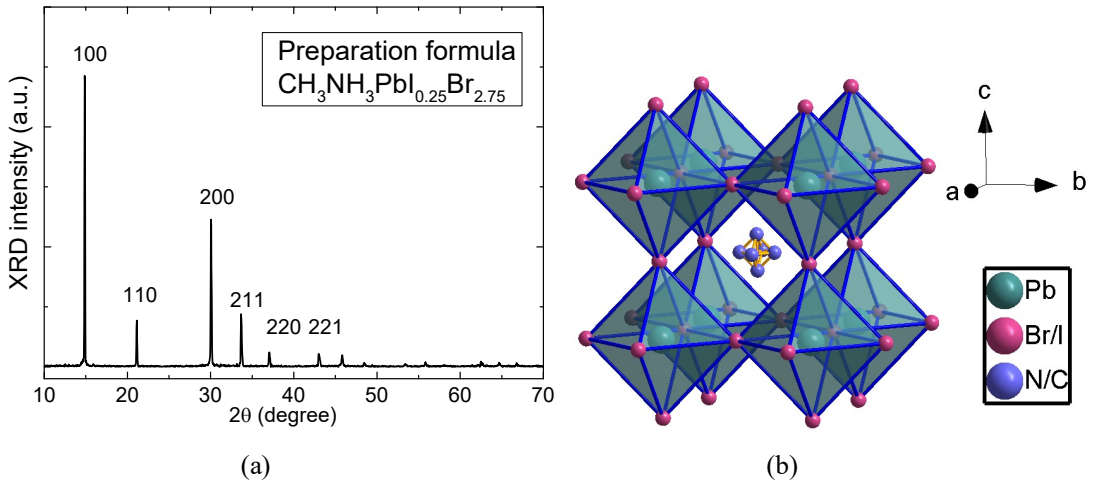

Fig. 5. (a) Experimental XRD pattern of preparation formula $CH_3NH_3PbI_2Br$ powder, and (b) corresponding SCXRD refined structure model of $CH_3NH_3PbI0.13Br2.87$ single crystal with cubic structure. Six possible positions, equally occupied by C or N, related through different symmetry operations, are presented. Hydrogen atoms were not added for the refinement.

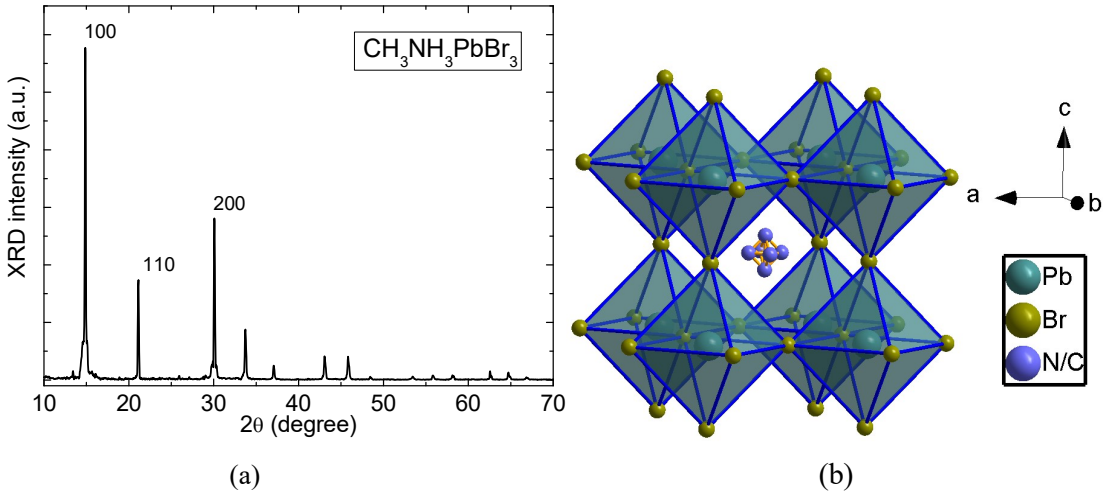

Fig. 6. (a) Experimental XRD pattern of $CH_3NH_3PbBr_3$ powder, and (b) corresponding SCXRD refined structure model of $CH_3NH_3PbBr_3$ single crystal with cubic structure. Six possible positions, equally occupied by C or N, related through different symmetry operations, are presented. Hydrogen atoms were not added for the refinement.

Fig. 7 shows the comparison between the experimental XRD patterns taken on perovskite powder samples and the reconstructed XRD patterns from the results of SCXRD adjustment. The

results suggest a good agreement between the experimental and simulation patterns, thus implying the correctness of lattice parameters shown in Table 1.

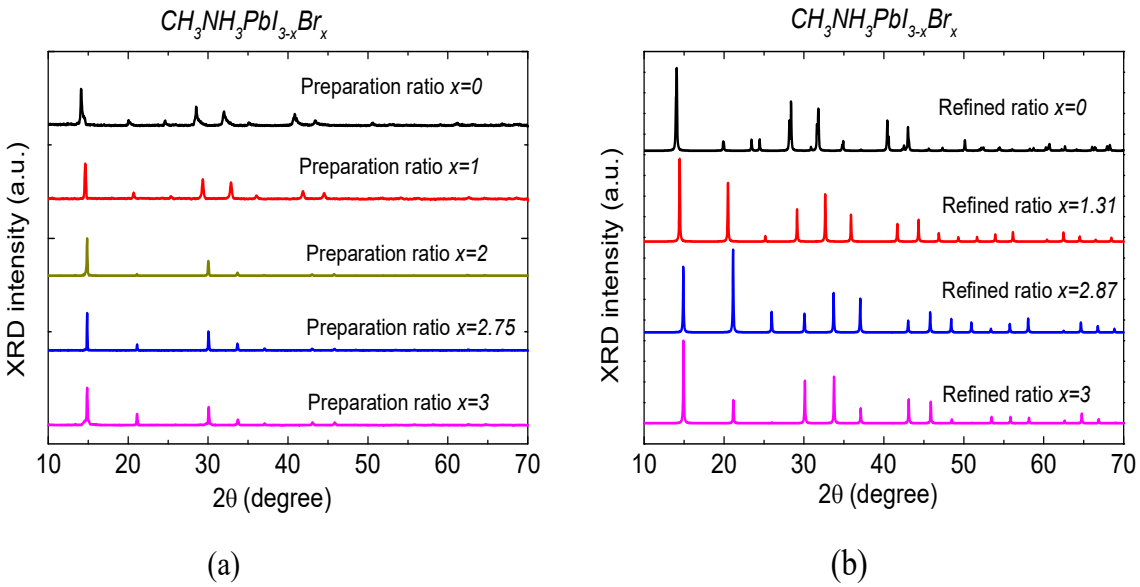

Fig. 7. (a) Experimental XRD patterns of $CH_3NH_3PbI_{3-x}Br_x$ powder, and (b) reconstructed powder XRD patterns from SCRXD analysis (note that the preparation ratio value x = 2 is missing).

IV. CONCLUSION

In summary, we have successfully carried out the growth of bulk single crystals of methylammonium lead mixed halide perovskites $CH_3NH_3PbI_{3-x}Br_x$ by two methods: (i) inverse temperature crystallization and (ii) anti-solvent diffusion. The obtained $CH_3NH_3PbI_{3-x}Br_x$ single crystals have been characterized by optical microscope as well as single crystal and powder X-ray diffraction. The color of bulk single crystals changes from black to orange depending on the concentration of bromide element in the compounds. The X-ray diffraction confirmed the tetragonal structure for $CH_3NH_3PbI_3$; and the structure became cubic with the bromide concentration higher than 1, starting from $CH_3NH_3PbIBr_2$, even though the surface morphology of those single crystals exhibit parallelogram shapes. The single crystal X-ray diffraction analysis reveals the positions of lead and halide atom in the unit cell. The orientations of the organic cation CH_3NH_3+ in the unit cell are clearly resolved.

ACKNOWLEDGMENT

This research is funded by the Vietnam National University, Hanoi (VNU) under project number QG.17.26.

REFERENCES

[1] M. A. Green, Y. Hishikawa, W. Warta, E. D. Dunlop, D. H. Levi, J. Hohl-Ebinger and A. W. H. Ho-Baillie, *Prog. Photovoltaics Res. Appl.* **25** (2017) 668.

[2] S. D. Stranks, S. D. Stranks, G. E. Eperon, G. Grancini, C. Menelaou, M. J. P. Alcocer, T. Leijtens, L. M. Herz, A. Petrozza and H. J. Snaith, *Science* **342** (2014) 341.

[3] O. Malinkiewicz, A. Yella, Y. H. Lee, G.M. Espallargas, M. Graetzel, M. K. Nazeeruddin, H. J. Bolink, *Nat. Photonics* **8** (2013) 128.

[4] G. Xing, N. Mathews, S. Sun, S.S. Lim, Y.M. Lam, M. Gratzel, S. Mhaisalkar, T.C. Sum, 'Long-Range Balanced Electron- and Hole-Transport Lengths in Organic-Inorganic $CH_3NH_3PbI_3$', Science. 342 (2013) 344–347.

[5] G. E. Eperon, S. D. Stranks, C. Menelaou, M. B. Johnston, L. M. Herz, H. J. Snaith, *Energy Environ. Sci.* **7** (2014) 982.

[6] J. W. Lee, H. S. Kim and N. G. Park, *Acc. Chem. Res.* **49** (2016) 311.

[7] M. Xiao, F. Huang, W. Huang, Y. Dkhissi, Y. Zhu, J. Etheridge, A. Gray-Weale, U. Bach, Y.-B. Cheng, L. Spiccia, *Angew. Chemie Int. Ed.* **53** (2014) 9898.

[8] N. J. Jeon, J. H. Noh, Y. C. Kim, W. S. Yang, S. Ryu, S. Il Seok, *Nat. Mater.* **13** (2014) 897.

[9] J. Burschka, N. Pellet, S.-J. Moon, R. Humphry-Baker, P. Gao, M. K. Nazeeruddin and M. Grätzel, *Nature* **499** (2013) 316.

[10] W. Nie, H. Tsai, R. Asadpour, J.-C. Blancon, A. J. Neukirch, G. Gupta, J. J. Crochet, M. Chhowalla, S. Tretiak, M. A. Alam, H.-L. Wang, A. D. Mohite, *Science* **347** (2015) 522.

[11] Y. Yang, S. Feng, M. Li, W. Xu, G. Yin, Z. Wang, B. Sun, X. Gao, *Sci. Rep.* **7** (2017) 46724.

[12] D. Liu, L. Wu, C. Li, S. Ren, J. Zhang, W. Li, L. Feng, Y. Road, *ACS Appl. Mater. Interfaces.* **7** (2015) 16330.

[13] D. Shi, V. Adinolfi, R. Comin, M. Yuan, E. Alarousu, A. Buin, Y. Chen, S. Hoogland, A. Rothenberger, K. Katsiev, Y. Losovyj, X. Zhang, P.A. Dowben, O.F. Mohammed, E.H. Sargent, O.M. Bakr, *Science* **347** (2015) 519.

[14] M. I. Saidaminov, A. L. Abdelhady, B. Murali, E. Alarousu, V. M. Burlakov, W. Peng, I. Dursun, L. Wang, Y. He, G. Maculan, A. Goriely, T. Wu, O. F. Mohammed and O. M. Bakr, *Nat. Commun.* **6** (2015) 7586.

[15] Takeo Oku, *Solar Cells - New Approaches and Reviews*, InTech, 2015.